Journal of Sound and Vibration (2001) **248**(1), 105–121
doi:10.1006/jsvi.2001.3731, available online at http://www.idealibrary.com on IDEAL®

AN EXPERIMENTAL INVESTIGATION OF THE AEROACOUSTICS OF A TWO-DIMENSIONAL BIFURCATED SUPERSONIC INLET

S.-M. Li, C. A. Hanuska and W. F. Ng

Mechanical Engineering Department Virginia Tech, MC 0238, *Blacksburg VA* 24061, *U.S.A.*

(*Received* 28 *August* 2000, *and in final form* 30 *March* 2001)

An experiment was conducted on a two-dimensional bifurcated, supersonic inlet to investigate the aeroacoustics at take-off and landing conditions. A 104·1 mm (4·1 in) diameter turbofan simulator was coupled to the inlet to generate the noise typical of a turbofan engine. Aerodynamic and acoustic data were obtained in an anechoic chamber under ground-static conditions (i.e., no forward flight effect). Results showed that varying the distance between the trailing edge of the bifurcated ramp of the inlet and the fan face had negligible effect on the total noise level. Thus, one can have a large freedom to design the bifurcated ramp mechanically and aerodynamically, with minimum impact on the aeroacoustics. However, the effect of inlet guide vanes' (IGV) axial spacing to the fan face has a first order effect on the aeroacoustics for the bifurcated 2-D inlet. As much as 5 dB reduction in the overall sound pressure level and as much as 15 dB reduction in the blade passing frequency tone were observed when the IGV was moved from 0·8 chord of rotor blade upstream of the fan face to 2·0 chord of the blade upstream. The wake profile similarity of the IGV was also found in the flow environment of the 2-D bifurcated inlet, i.e., the IGV wakes followed the usual Gauss' function.

1. INTRODUCTION

The first successful civilian supersonic aircraft, the Concorde, was introduced by Air France and British Airways in the 1970s. From the Concorde's beginning, the environmental impact of its engine noise has been questioned. Many countries and airports have restricted the frequency of its flights due to take-off and landing noise. The governmental limitations of the Concorde due to the noise pollution problem and other factors have reduced the financial returns of the Concorde. A recent renewed interest in a commercial supersonic aircraft has led NASA to begin a High Speed Civil Transport (HSCT) research program [1]. One of the most important objectives of HSCT is to develop a more economically viable aircraft than the Concorde. One of the concerns among others is the noise level at the aircraft take-off and landing conditions. At these conditions, forward propagated fan noise becomes a more noticeable contributor to the airport community noise levels. As a result, the inlet becomes a significant component for noise generation and propagation of an aircraft.

A bifurcated two-dimensional (2-D) supersonic inlet is one of the several inlets being considered for the HSCT program. The bifurcated 2-D inlet design incorporates a rectangular inlet opening that gradually changes to a circular cross-section at the fan face. The bifurcation ramp or splitter plate center body is adjustable to obtain the appropriate shock wave conditions with the inlet for the engine at transonic and supersonic flights. With

0022-460X/01/460105 + 17 $35.00/0

the adjustable center body, the flow condition at the fan face can also be controlled at a subsonic condition. The bifurcated 2-D inlet also incorporates inlet guide vanes right in front of the fan face.

The bifurcated 2-D, supersonic inlet, as compared with either a subsonic or an axisymmetric supersonic inlet, has more complicated and variable features in order to be able to perform at subsonic, transonic and supersonic speeds. The effects of these features on the noise generation and propagation involve more complicated phenomena and need to be investigated thoroughly to fully understand the individual acoustic effects of each feature.

Unfortunately, publications of aeroacoustic research on bifurcated 2-D supersonic inlets in the literature are very limited. An older version of a bifurcated 2-D supersonic inlet, designed by NASA was tested by Wagner [2]. The NASA-designed bifurcated 2-D inlet did not have IGV. Since the tests were conducted at ground-static conditions and the inlet did not have a bellmouth, a significant boundary layer separation was recorded at the cowl lip. Miller [3] made continued effort to examine the performance of the NASA-designed bifurcated 2-D inlet without IGV. His tests were ground-static too but conducted with a bellmouth to reduce the cowl lip boundary layer separation. Both work documented the aeroacoustic and aerodynamic performance of the bifurcated 2-D supersonic inlets at two different fan speeds. Comparisons were made between the performances of the bifurcated 2-D supersonic inlets and the axisymmetric supersonic inlets. Hanuska [4] conducted another aeroacoustic experiment for a new bifurcated 2-D supersonic inlet with IGV. This bifurcated 2-D supersonic inlet, designed recently by Boeing Company, differed from the old NASA designed inlet in that the Boeing bifurcated 2-D supersonic inlet had IGV. In Hanuska's work [4], the concern was to evaluate the use of flat plate IGV and airfoil IGV on the effects of "soft choking" to reduce noise.

The above-mentioned publications are the only few ones available for bifurcated 2-D supersonic inlets. Many basic features of the bifurcated 2-D supersonic inlets are not explored. Of particular interests are the effects on the aeroacoustics of varying the distance between the trailing edge of the bifurcated ramp and the fan face, as well as the acoustic effect of IGV axial spacing to the fan face in the environment of the bifurcated 2-D inlet. The work in this paper will focus on these two effects, at the conditions corresponding to aircraft take-off and landing approach.

It should be mentioned that there are a few publications on the experimental research of the aeroacoustics on IGV/rotor or wakes/rotor interactions, such as Trunzo *et al.* [5], Cudina [6], Johnston and Fleeter [7], etc. However, none of the research was completed with a bifurcated 2-D supersonic inlet. It has been pointed out by Johnston and Fleeter [7] that wakes/rotor interactions are "the most common and least understood source of unsteady aerodynamic excitation". Therefore, it is believed that the aeroacoustic data of wakes/rotor interactions with a bifurcated 2-D inlet will add to the understanding of the physics of this kind of unsteady aerodynamic excitation.

2. EXPERIMENTAL TECHNIQUES

This section describes the inlet, turbofan simulator and test set-up which utilized the Virginia Tech Anechoic Chamber in the Vibration and Acoustics Laboratory. The same facilities have been used in the past by Nuckolls and Ng [8].

2.1. BIFURCATED 2-D INLET

The tested bifurcated 2-D inlet was designed by Boeing Company and was scaled to match with a 104·1 mm (4·1 in) diameter turbofan simulator. The inlet was designed

for a cruise speed of Mach number 2·7 and incorporated an adjustable splitter plate or bifurcated ramp that allows the throat area to be changed. The splitter plate is able to collapse and expand to maintain the correct shock wave structure during transonic and supersonic flight or to control the engine mass flow rate in subsonic flight. The inlet is mounted on the aircraft wing with the splitter plate oriented vertically. Another distinguishing element of the bifurcated 2-D inlet design is the rectangular inlet opening that gradually transforms to the circular cross-section at the fan face. The bifurcated 2-D inlet used for this research, as shown in Figures 1 and 2 of the cutaway drawings, does not incorporate the adjustable splitter plate but uses a bifurcated ramp that is fixed at its take-off and landing conditions, fully collapsed. No auxiliary doors were used in these experiments although the inlet had provisions for doors to be added later. Because all the tests were performed at ground-static conditions, a bellmouth was applied to prevent separation at the cowl lip, as shown in Figures 1 and 2.

The bifurcated two-dimensional inlet was manufactured in two sections, such that the front of the inlet had the splitter plate fixed, while the back half had a slot for a removable rear splitter plate. The distance between the baseline splitter plate trailing edge and the fan face is equal to one fan diameter. A new splitter plate was made in which the distance between the trailing edge of the new splitter plate and the fan face is equal to half the fan diameter, rather than one fan diameter as for the baseline case.

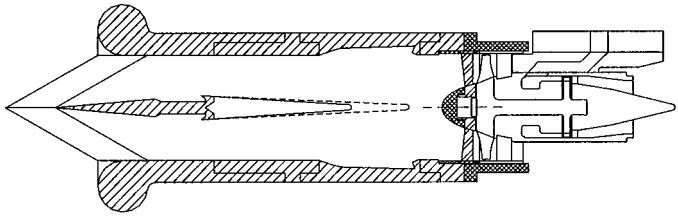

Figure 1. Comparison of the geometry of the baseline ramp and new ramp (dashed line).

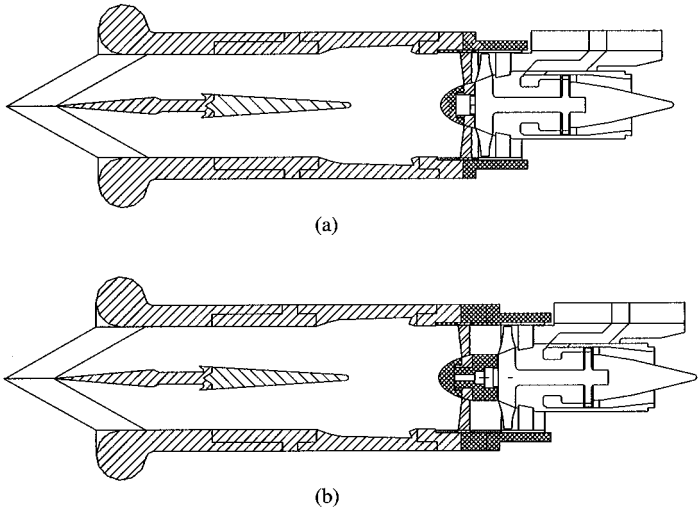

Figure 2. Comparison of the geometry of (a) the baseline and (b) modified IGV axial spacings.

The bifurcated 2-D inlet also incorporated IGV. The IGV assembly consisted of a hoop ring, 14 flat plate IGV and a nose cone (see Figure 1). The hoop ring supported the IGV and the nose cone. The stainless-steel IGV were 0·79 mm (1/32 in) flat plates with a decreasing chord length from 11·6 mm (0·457 in) at the fan outer casing to 7·6 mm (0·30 in) at the fan hub. The baseline IGV were positioned 0·8 chord of the fan blade upstream of the fan face (measured at the mid-span of the IGV). A new spacer was designed to fit between nose cone and the fan face so that the modified IGV distance was moved to 2 chords of the fan blade upstream of the fan face (again measured at the mid-span of IGV), as shown in Figure 2.

2.2. TURBOFAN SIMULATOR

The noise source used in this experiment was a Tech Development Model 460 turbofan simulator. This simulator functions like a fan in a high-bypass ratio aircraft engine. Figure 1 shows the simulator mated to the inlet. The simulator was powered by high-pressure air exhausting through a single-stage turbine. The turbine turns a single-stage fan, drawing air into the simulator from the ambient atmosphere. The turbine and fan air streams are mixed downstream of the simulator exit. The 104·1 mm (4·1 in) diameter fan was made up of 18 blades and 26 outlet guide vanes. The Model 460 has a design speed of 80 000 r.p.m., and was designed to be capable of producing a total pressure ratio of 1·6 with a mass flow of 1·23 kg/s (2·72 lb m/s). For these experiments, the simulator was tested at 59 400 and 65 600 r.p.m., simulating the aircraft landing and take-off conditions.

2.3. TEST FACILITY

All testing was performed at the Virginia Tech Anechoic Chamber. All experiments conducted were ground-static tests. The chamber working space dimensions are $4 \times 2{\cdot}7 \times 2$ m. This space is surrounded by sound absorbing wedges made of industrial fiberglass. This facility is considered anechoic for frequencies above 200 Hz with an ambient noise level of approximately 30 dB. This ambient noise level is considerably lower than the noise levels of interest measured during testing. The turbofan simulator was connected and supported firmly at the three directions, from the ground, from the roof, and from the wall, so that the vibration signal of the ground and the anechoic chamber in noise spectra was negligible. The turbofan simulator was mounted 4 ft above the ground level to prevent the ingestion of ground vortex.

2.4. AERODYNAMIC MEASUREMENTS

Steady state pressure measurements were taken at several locations of the bifurcated 2-D inlet to document the flow condition. A Pitot-static probe of diameter 1·6 mm (0·0625 in) was used to measure static and total pressures in front of the fan face. The Mach number was calculated from the relation between total pressure, static pressure, and the Mach number. At the fan exit, a Kiel probe was used to measure the total pressure.

With the IGV assemblies fitted directly in front of the fan face, it was difficult to measure the wakes behind the IGV. For pressure measurements behind the IGV, a spacer ring was placed which moved the inlet IGV away from the fan face. The measurement locations placed the Pitot-static probe head at the same distance from the trailing edge of the IGV to that of the fan face. The bifurcated 2-D inlet aerodynamic measurement configuration and locations are illustrated in Figure 3. All these measurement locations are chosen to give

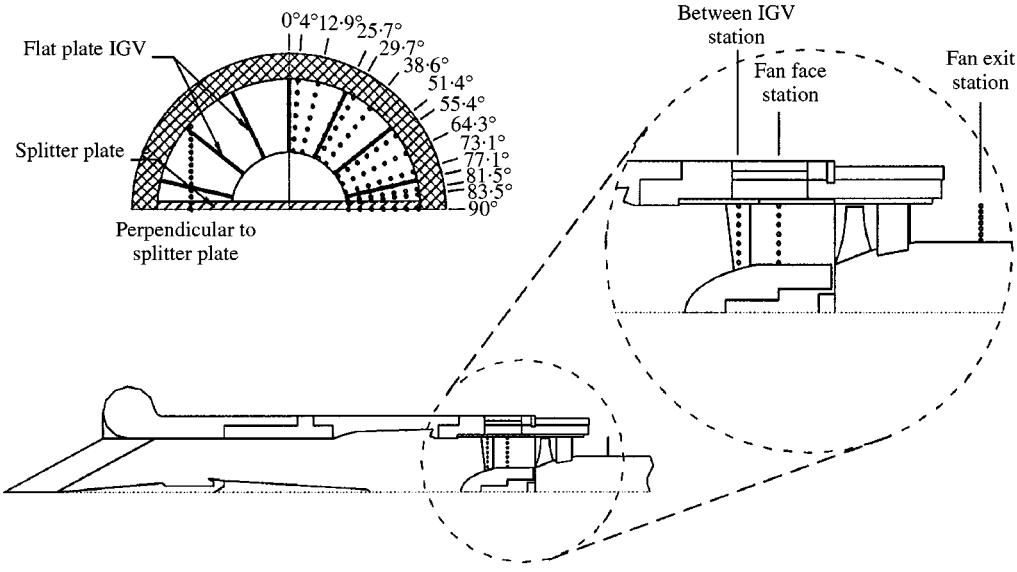

Figure 3. Locations of aerodynamic measurements.

a complete flow contour at the fan face. The 13 circumferential measurement locations are 0, 4, 12·9, 25·7, 29·7, 38·6, 51·4, 64·3, 73·1, 77·1, 81·1, 83·5, and 90°. At each of the 13 circumferential measurement locations, the pressure was measured at seven equally spaced radial locations. For the fan face distributions, symmetry around an IGV for the measurement locations of 29·7 and 55·4° and symmetry by quadrant for the entire inlet were assumed. A midspan perpendicular traverse to both an IGV and the splitter plate was also performed at the fan face with a higher spatial resolution.

2.5. ACOUSTIC MEASUREMENTS

Acoustic measurements were taken at 12 points along a circular arc ranging from 0 to 110° at a horizontal distance of 1·22 m (48 in) from the cowl lip of the inlet. The microphone was elevated 1·22 m (48 in) from the floor for all measurements. Figure 4 illustrates the acoustic measurement locations.

A Bruel and Kjaer Model 4136 condenser microphone with a 6·4 mm (0·25 in) diameter diaphragm was used to measure the sound pressure level. The manufacturer calibrated the microphone from 0 to 200 000 Hz but the microphone was only linear from 0 to 30 000 Hz. For the frequencies above 30 000 Hz, the calibration curve provided by Bruel and Kjaer was used to correct the data. The signal from the microphone was directed into a Bruel and Kjaer Model 2639 pre-amplifier. A Hewlett Packard Model 8360 signal analyzer was used to acquire and process the acoustic signals from the microphone. The analyzer frequency range of 0–102 400 Hz and resolution of 800 lines gave a bandwidth of 128 Hz. From each of these spectra, the sound pressure levels (SPL) of the blade passing frequency (BPF) and first harmonic tone, and the overall sound pressure levels for the frequencies from 0 to 102 400 Hz were obtained. To account for the variation inherent to these acoustic measurements, 20 spectra were averaged to produce one measurement for a given position, configuration, and speed. Next, five of these measurements were taken and averaged to yield

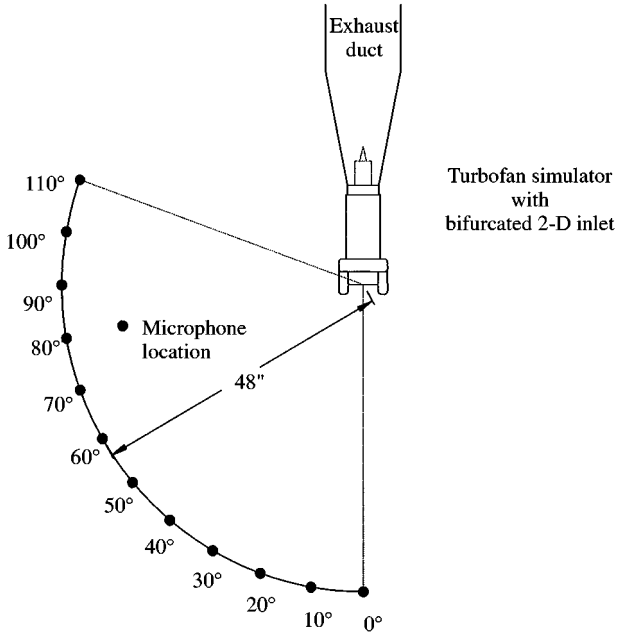

Figure 4. Locations of microphone measurements.

the sound pressure level for a particular position. In total, the sound pressure level was measured 100 times and averaged to yield each data point.

3. RESULTS AND DISCUSSION

3.1. FAN OPERATING CONDITIONS

The loading of the fan was controlled with the use of a choke plate at the fan exit. The area of the choke plate used in these experiments was selected to be smaller than the flow area through the IGV. This ensured that the loading of the fan was determined by the choke plate and not the IGV. The total pressure ratio was calculated using an area average of the measured pressure at the fan face and at the fan exit. The mass flow was calculated using an integration of the measurements at the fan face. The corrected average total pressure ratios and mass flows were 1·273 and 0·830 kg/s (1·823 lb m/s) at the speed of 59 400 r.p.m. and 1·343 and 0·925 kg/s (2·04 lb m/s) at the speed of 65 600 r.p.m. When compared with the fan performance map provided by the simulator manufacturer, the two operating points were found close to the middle of the region between the surge and choking curves.

3.2. FAN FACE FLOW DISTORTION

The performance of the bifurcated two-dimensional inlet was characterized by the amount of total pressure recovery and flow distortion at the fan face. The upstream disturbances of the turbofan engine created the circumferential gradients that increased the noise generation and decreased the compressor stability margin.

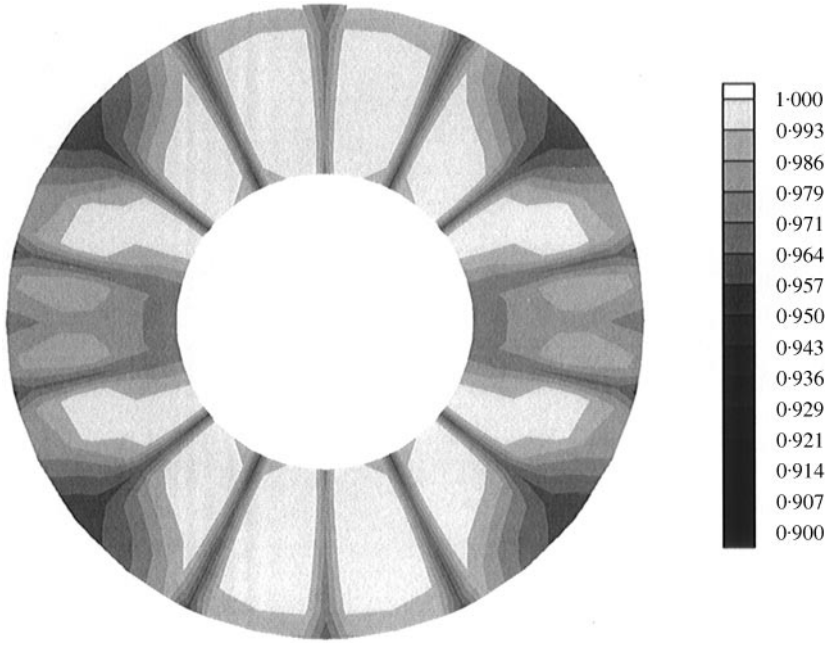

Figure 5. Fan face total pressure recovery at 59 400 r.p.m.

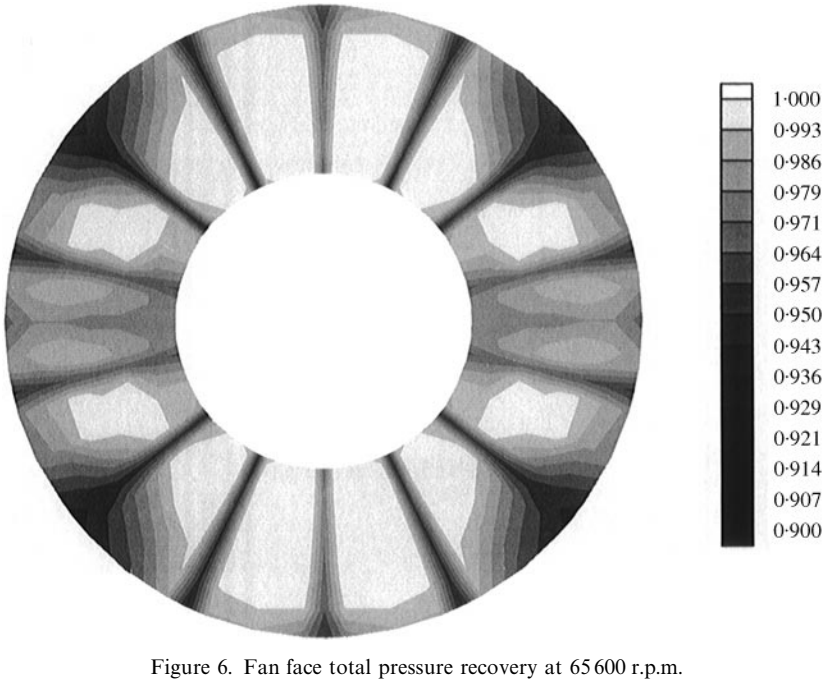

Figure 6. Fan face total pressure recovery at 65 600 r.p.m.

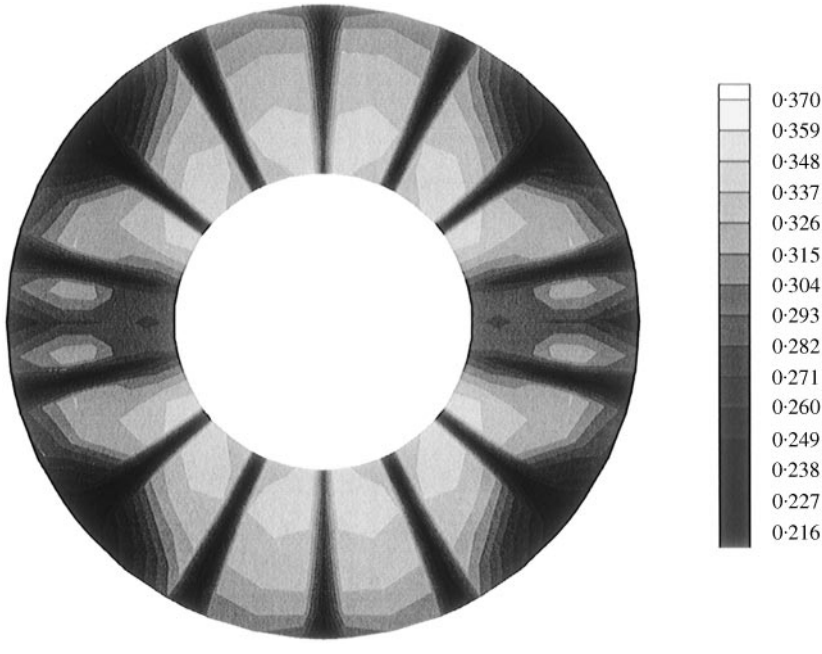

Figure 7. Fan face Mach number distribution at 59 400 r.p.m.

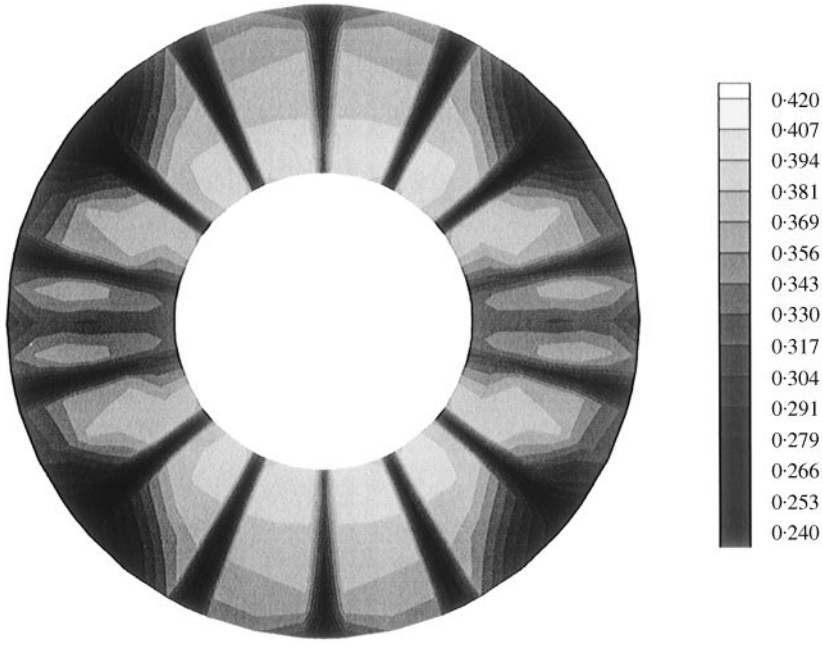

Figure 8. Fan face Mach number distribution at 65 600 r.p.m.

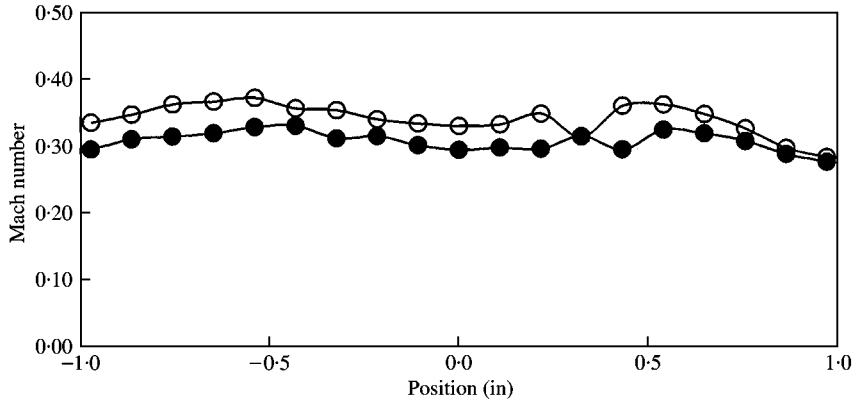

Figure 9. Splitter plate wake at 59 400 and 65 600 r.p.m. (○, 65 600 r.p.m.; ●, 59 400 r.p.m.).

In this paper, the total pressure contour is expressed by the total pressure recovery. The total pressure recovery is defined as a dimensionless total pressure normalized by the ambient pressure. The total pressure contours at the fan face for the speeds of 59 400 r.p.m. and 65 600 r.p.m. are given in Figures 5 and 6. Boundary layer losses were evident at the fan casing. The IGV caused 14 circumferential higher loss regions at the fan face. The splitter plate wake was visible at the horizontal plane. It was evident that the main circumferential distortion was from the wakes of IGV and not from the splitter plate. Figures 5 and 6 show that the flow losses were increased a little at higher speed. The area-averaged total pressure recovery was 0·986 and 0·983 for the speeds of 59 400 and 65 600 r.p.m., respectively.

The fan face Mach number distribution at 59 400 r.p.m., is shown in Figure 7. Again, the wakes of the 14 IGV and the splitter plate were clearly visible as areas of low Mach number. The main circumferential distortion was from the wakes of IGV and not from the splitter plate. As the rotational speed of the turbofan simulator was increased to 65 600 r.p.m., the core flow velocity increased and the wakes of the IGV became deeper, as shown in Figure 8.

The width and depth of the splitter plate and IGV wakes were further examined with traverses perpendicular to the splitter plate and one of the IGV separately. The influence of the splitter plate wake on the fan face distortion is illustrated by the midspan traverse perpendicular to the splitter plate in Figure 9. Because the trailing edge of the splitter plate for the baseline case was located upstream of the IGV and far upstream from the fan face, the wake was able to dissipate and become quite flat at the fan face.

It was noticed that the fan face was located as close as 42% of the ramp chord from the ramp trailing edge and the wake profile of the ramp was quite flat and hard to be recognized from the wake traverse measurements as compared with the IGV wake profile. A strong interaction may exist between the ramp wake and the IGV as well as IGV wakes. The ramp wake dissipated and became wide and flat at the fan face due to this strong interaction.

The width and depth of the IGV wakes were examined by a mid-span perpendicular traverse behind the IGV at the 0° position. Figure 10 presents the difference in wake between the two speeds. Because the diameter of the probe was larger than the inlet guide vane thickness, the actual IGV wake may have been deeper than shown.

A comparison of the wake profiles of the splitter plate in Figure 9 and IGV in Figure 10 shows that the distortion of the splitter plate wake at the fan face was negligible. It is

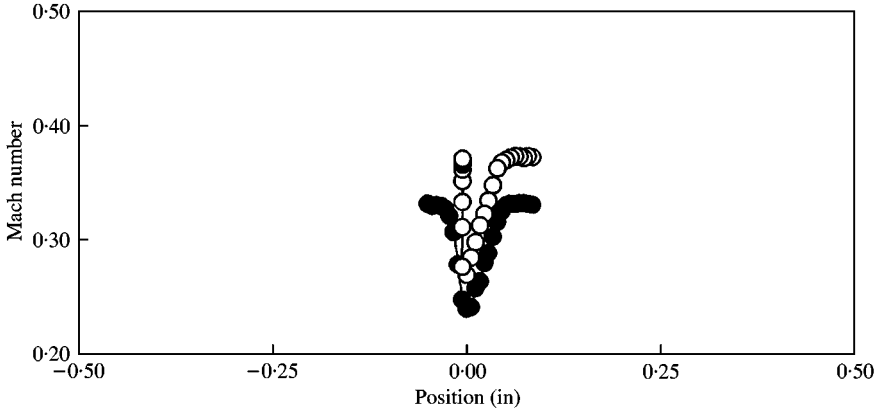

Figure 10. IGV wake at 59 400 and 65 600 r.p.m. (○, 65 600 r.p.m.; ●, 59 400 r.p.m.).

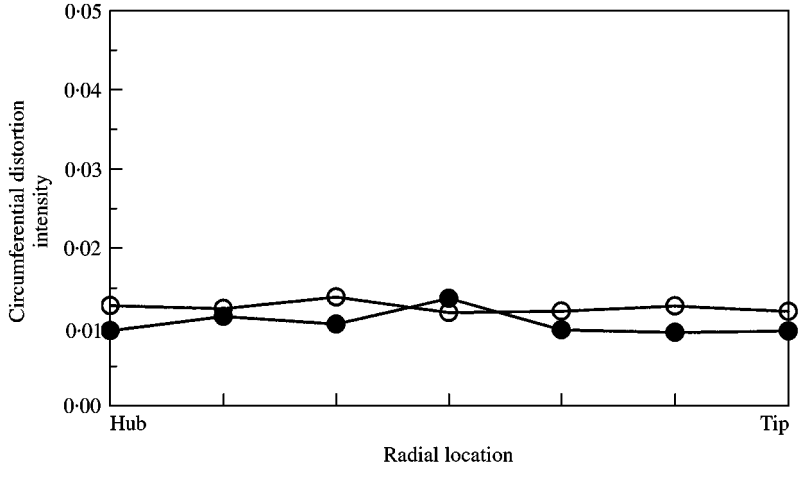

Figure 11. Fan face circumferential distortion (○, 65 600 r.p.m.; ●, 59 400 r.p.m.).

expected that the deeper IGV wakes generate higher noise than the shallow splitter plate wake.

The amounts of circumferential distortions were further quantified according to the ARP [9] standard. A comparison between the circumferential distortion intensity for each annular ring at different radial locations is given in Figure 11. It illustrates that the amount of circumferential distortion was quite constant in the radial direction. As the speed increased, the circumferential distortion increased at almost all radial locations.

Experimental evidence has shown that a similarity in streamline velocity profiles for the wakes behind flat plates, circular cylinders, isolated airfoils, and rotor blade wakes exists [1]. Using the same data correlation technique described by Reynolds *et al.* [10], the similarity rule has been examined for the IGV wake measurements, reported in this paper, in the environment of the 2-D inlet. As shown in Figure 12, the similarity was found at two different speeds tested with the flat plate IGV, under the condition of the upstream ramp

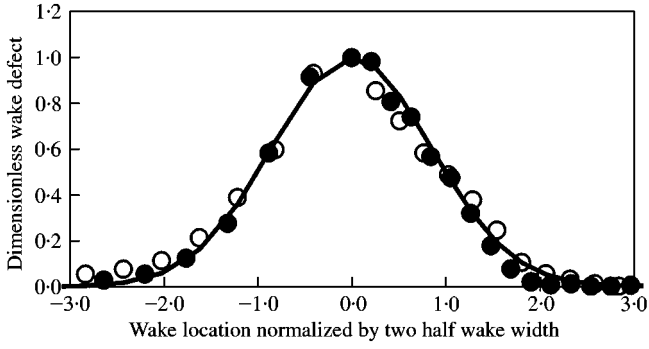

Figure 12. Wake similarity for 2-D inlet IGV (○, 65 600 r.p.m.; ●, 59 400 r.p.m.; ——, Reynolds [10]).

wake interaction in the 2-D bifurcated inlet, i.e., the IGV wakes followed the same Gauss' function $\exp(-0{\cdot}693\eta^2)$.

The wake decay has been examined by using several correlations presented in the same paper of Reynolds *et al.* [10]. Reynolds *et al.* described three different wake decay correlations. One was for isolated airfoils, and the other two was for cascades and rotor wakes respectively. The three decay correlations were applied separately to calculate the wake decay of the 2-D inlet IGV between the two tested locations. The changes of the maximum velocity defects between the two locations were found around one-third based on the three correlations. The correlation for cascades gave the maximum change of the maximum velocity defect of 35%, while the correlation for rotor wakes gave the smallest change of 31%. As there was strong interaction of the upstream ramp wake with the downstream IGV and IGV wakes in the 2-D bifurcated inlet, one could not expect the three correlations to give good prediction for this decay.

On the other hand, a few typical computational aeroacoustics codes were available, which were based on both an annular inlet geometry model to simulate the casing of the fan and a wake decay model to account for the wake decay. It is obvious that the sound propagation and cut-off frequency in an annular geometry are different from those in the rectangular inlet. For the additional bifurcated center body and the strong interaction between the ramp wake and IGV as well as the IGV wakes, the available computational aeroacoustics codes need some modification for the prediction of the fan noise with the 2-D bifurcated inlet at different IGV spacing. Bearing these points in mind, in this paper, no attempt was made to apply the available codes to predict the sound characteristics of the 2-D inlet.

3.3. ACOUSTIC EFFECTS OF IGV AXIAL SPACING AT LANDING CONDITION

Two sample acoustic spectra to compare the effect of IGV spacing are shown in Figure 13. The spectra were taken with the turbofan engine simulator moving at 59 400 r.p.m., and the microphone was located at 50° location. As is common among fans with subsonic blade tip velocities, the blade passing tone dominated the spectra at about 18 kHz. The first harmonic of the blade passing frequency was also prominent at around 36 kHz. As expected, the modified IGV spacing reduced the blade passing tone SPL significantly. The modified IGV spacing had little effect on the broadband noise.

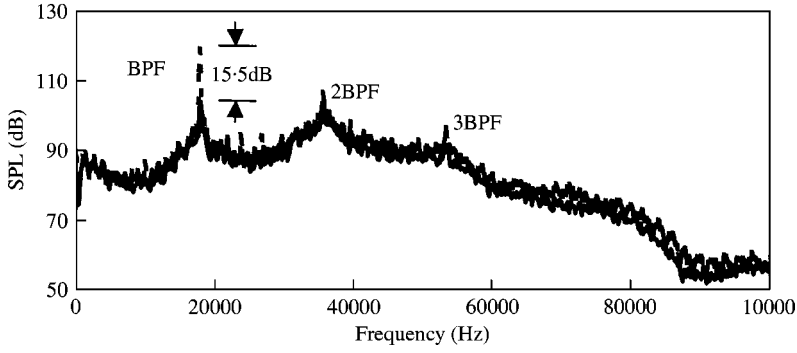

Figure 13. Typical spectra comparing baseline and modified IGV axial spacings at 50° microphone location and 59 400 r.p.m., fan speed (- - -, baseline; ——, modified).

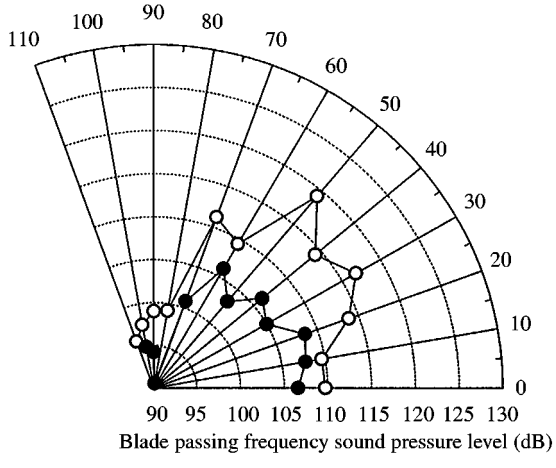

Figure 14. Comparison of the directivity of blade-passing-frequency tone at 59 400 r.p.m. fan speed for different IGV axial spacing (○, baseline; ●, modified).

The key results of the experiment are presented in directivity plots. Figure 14 shows the effects of IGV spacing on the radiated tone at 59 400 r.p.m. The significant reduction of the tone SPL was noticed at most locations. There was a maximum reduction of 15·5 dB in the tone SPL at the 50° location. Between 20 and 90° positions, the average reduction was 8·5 dB in tone SPL.

Figure 15 shows the effect of IGV spacing on the first harmonic of the BPF tone at 59 400 r.p.m. The reduction in the first harmonic of the BPF tone was quite evident, as high as 6 dB.

Figure 16 shows the effect of IGV spacing on the overall sound pressure level at 59 400 r.p.m. On average, the overall SPL was reduced by approximately 3 dB for all angular positions, with as much as 4·5 dB average reduction between 30 and 70°.

3.4. ACOUSTIC EFFECTS OF IGV AXIAL SPACING AT TAKE-OFF CONDITION

Results for the take-off condition at 65 600 r.p.m., are presented in Figures 17–19. Figures 17–19 show the comparison of the directivity of BPF tone, first harmonic of the

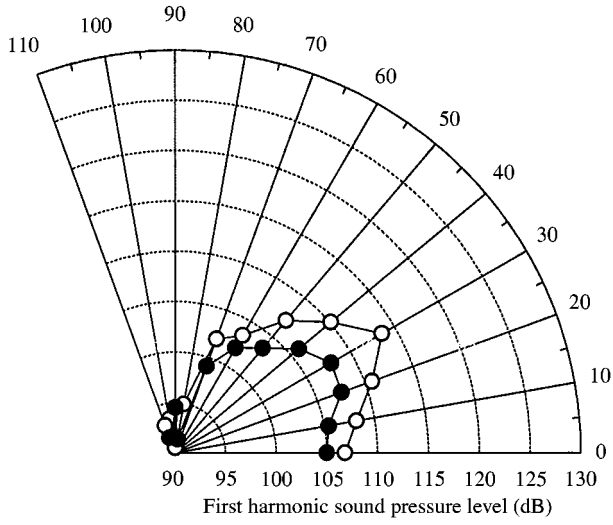

Figure 15. Comparison of directivity of the first harmonic of the blade-passing-frequency time at 59 400 r.p.m. fan speed for different IGV axial spacing (○, baseline; ●, modified).

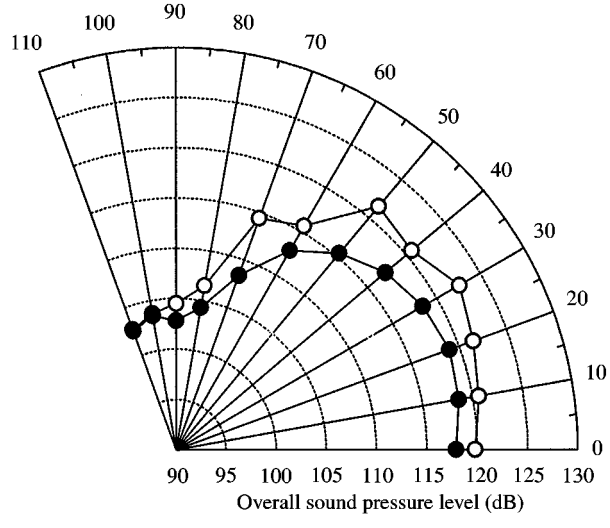

Figure 16. Comparision of directivity of the overall sound pressure level at 59 400 r.p.m. fan speed for different IGV axial spacing (○, baseline; ●, modified).

BPF tone, and the overall sound pressure level respectively. It can be seen from Figure 17 that a significant reduction of the tone SPL was also noticed at most locations. There was a maximum reduction of 8·2 dB in the tone SPL at the 0° location, fan axial location. Between 0 and 70° positions, the average reduction was 6·3 dB in tone SPL.

Figure 18 shows the effect of IGV spacing on the first harmonic of the BPF tone at 65 600 r.p.m. The reduction in the first harmonic of the BPF tone was quite evident too, as high as 6·8 dB at 30° position.

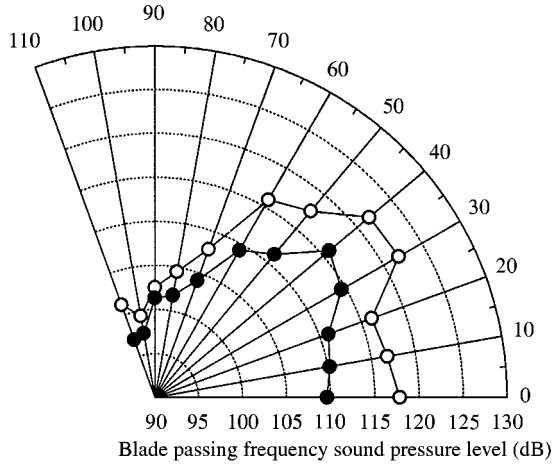

Figure 17. Comparison of the directivity of blade-passing-frequency tone at 65 600 r.p.m. fan speed for different IGV axial spacing (○, baseline; ●, modified).

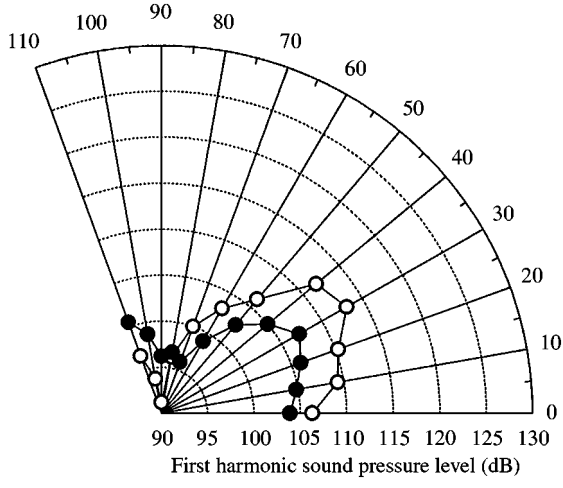

Figure 18. Comparison of the directivity of the first harmonic of the blade-passing-frequency tone at 65 000 r.p.m. fan speed for different IGV axial spacing (○, baseline; ●, modified).

Figure 19 shows the effect of IGV spacing on the overall sound pressure level at 64 600 r.p.m. On average, the overall SPL was reduced by 3·2 dB for all angular position, with as much as 4·7 dB reduction between 30 and 70°.

As compared with an axisymmetric inlet, the noise reduction with different IGV spacing from the fan face may be more significant in the case of the 2-D inlet due to the strong interaction of the upstream ramp wake with the downstream IGV wakes and a possibly much faster decay of the IGV wakes. It is also worth a further examination to see if the characteristics of the sound propagation and frequency cut-off in the 2-D inlet are another key factor for this significant noise reduction.

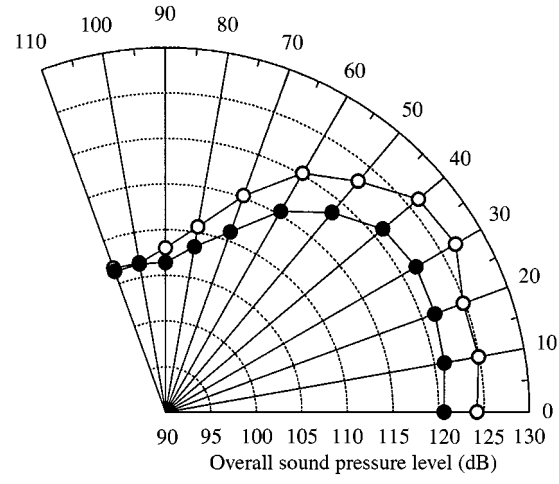

Figure 19. Comparison of the directivity of the overall sound pressure level at 65 000 r.p.m. fan speed for different IGV axial spacing (○, baseline; ●, modified).

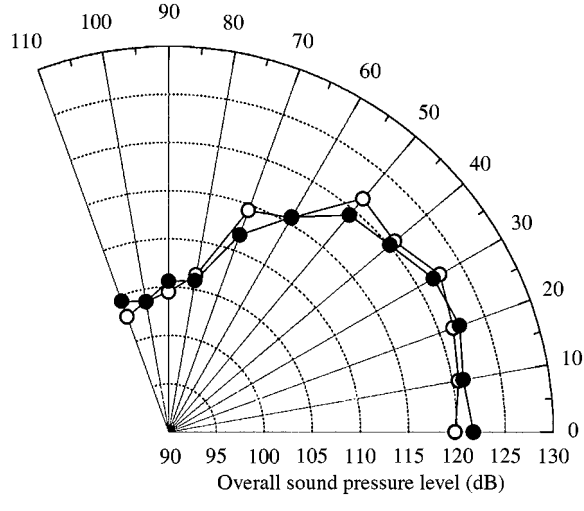

Figure 20. Comparison of the directivity of the overall sound pressure level at 59 400 r.p.m. fan speed for different ramp axial spacing (○, baseline; ●, modified).

3.5. ACOUSTIC EFFECTS OF RAMP AXIAL SPACING

The acoustic effect due to different axial ramp spacing was almost negligible at the baseline IGV spacing. The results for the overall sound pressure level directivity plots are shown in Figures 20 and 21 at approach and take-off conditions respectively. It can be seen from Figures 20 and 21 that no measurable effect was obtained due to different axial spacing of the inlet ramp. These acoustic results are consistent with results from the aerodynamic measurements of the baseline. It is shown that the wake of the closer spacing of the inlet ramp is negligible for the noise generation as compared with the IGV wakes. This will give much larger freedom to design the inlet ramp aerodynamically and mechanically.

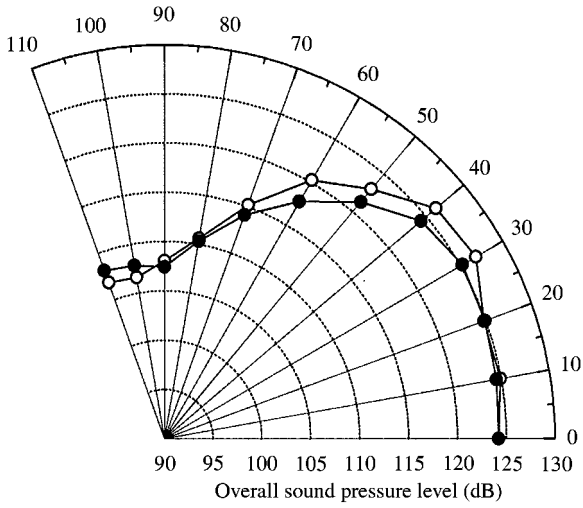

Figure 21. Comparison of the directivity of the overall sound pressure level at 65 600 r.p.m. fan speed for different axial spacing (○, baseline; ●, modified).

It should be mentioned that the above results have been obtained with the IGV at 0·8 chord of the fan face. As the ramp is always far from the fan face as compared with the IGV location, it is expected that the ramp wake should become more uniform at the fan face with the bigger IGV spacing and the acoustic effect due to the different axial ramp spacing will also be negligible in the case of increased IGV spacing.

4. CONCLUSIONS

An experiment was conducted on a two-dimensional bifurcated, supersonic inlet to investigate the aeroacoustics of varying the distance between the trailing edge of the ramp and the fan face, as well as changing the IGV axial spacing to the fan face. Experiments were conducted at landing and take-off conditions. A 104·1 mm (4·1 in) diameter turbofan simulator was coupled to the inlet to generate the noise source typical of a turbofan engine. Acoustic data were obtained in an anechoic chamber under ground-static conditions. Results showed that varying the distance between the trailing edge of the ramp and the fan face had negligible effect on the total noise level. The wake of the bifurcated center body in the 2-D inlet dissipated and became wide and shallow, so that it was hard to be recognized as a wake profile at the fan face for the baseline. A strong interaction of the ramp wake with IGV and IGV wakes were evident. One can have a large freedom to design the inlet ramp aerodynamically and mechanically, without consideration of its acoustic effects. However, the inlet guide vanes axial spacing to the fan face has a first order effect. As much as 5 dB reduction in the overall sound pressure level and as much as 15 dB reduction in the blade passing frequency tone were observed when the IGV was moved from 0·8 chord of rotor blade upstream of the fan face to 2·0 chord upstream. In addition, the wake profile similarity was found for the flat plate IGV in the environment of the 2-D bifurcated inlet, i.e., the IGV wakes followed the usual Gauss' function.

ACKNOWLEDGMENT

This work was supported by NASA Glenn Research Center, technical monitor, Mr Woodie Woodward. Both the financial support and the technical interchanges with Mr Woodward are most gratefully acknowledged. The authors would like to thank Mr William Stinnet for his assistance in the long hours of experiments in taking data.

REFERENCES

1. R. O. CARDEN 1994 *The Virginia Engineer* **33**, 11–12. Nation's largest aircraft firms team up to develop SST systems.
2. R. WAGNER 1995 *M.S. Thesis*, *Virginia Polytechnic Institute and State University*. Aeroacoustics of the bifurcated 2 D supersonic inlet.
3. K. C. MILLER 1996 *M.S. Thesis*, *Virginia Polytechnic Institute and State University*. Comparison of the aeroacoustics of two small-scale supersonic inlets.
4. C. A. HANUSKA 1998 *M.S. Thesis*, *Virginia Polytechnic Institute and State University*. Aeroacoustic effect of choking at inlet guide vanes in subsonic and supersonic inlets.
5. R. TRUNZO, B. LAKSHMINARAYANA and D. E. THOMPSON 1981 *Journal of Sound and Vibration* **76**, 233–259/0022-460x/81/100233 + 27. Nature of inlet turbulence and strut flow disturbances and their effect on turbomachinery rotor noise.
6. M. CUDINA 1992 *Noise Control Engineering Journal* **39**, 21–310. Noise generated by a vave-axial fan with inlet guide vanes.
7. R. JOHNSTON and S. FLEETER 1998 *AIAA Paper*, AIAA-98-3896, 34th AIAA/ASME/SAE/ASEE Join Propulsion Conference & Exhibit. Three-dimensional time resolved measurements of IGV-rotor potential interactions.
8. W. E. NUCKOLLS and W. F. NG 1995 *American Society of Mechanical Engineers Journal of Engineering for Gas Turbines and Power* **117**, 237–244. Fan noise reduction from a supersonic inlet during simulated aircraft approach.
9. ARP 1978 *Technical Report* 1420, Society of Automotive Engineers, Inc. Gas turbine engine inlet flow distortion guidelines.
10. B. REYNOLDS, B. LAKSHMINARAYANA and A. RAVINDRANATH 1979 *American Institute of Aeronautics and Astronautics Journal* **17**, 959–967/aiaaj78-1141R. Characteristics of the near wake of a compressor of a fan rotor blade.